

# Multispectral Palmprint Recognition Using a Hybrid Feature

*Sina Akbari Mistani, Shervin Minaee and Emad Fatemizadeh*

Electrical and Computer Engineering Department, New York University, USA.

## ABSTRACT

Personal identification problem has been a major field of research in recent years. Biometrics-based technologies that exploit fingerprints, iris, face, voice and palmprints, have been in the center of attention to solve this problem. Palmprints can be used instead of fingerprints that have been of the earliest of these biometrics technologies. A palm is covered with the same skin as the fingertips but has a larger surface, giving us more information than the fingertips. The major features of the palm are palm-lines, including principal lines, wrinkles and ridges. Using these lines is one of the most popular approaches towards solving palmprint recognition problem. Another robust feature is the wavelet energy of palms. In this paper we used a hybrid feature which combines both of these features. At the end, minimum distance classifier is used to match test images with one of the training samples. The proposed algorithm is tested on a well-known multispectral palmprint dataset and achieved an average accuracy of 98.8%.

## 1. INTRODUCTION

Personal identification has always been required in critical tasks and personal devices; The traditional tools for obtaining personal identification are password and ID cards, which are widely used today. However, besides common problems with memorizing passwords and keeping an ID card, they are exposed to being disclosed or stolen, threatening the security. Today, the area of personal identification is exploiting computer-aided systems as a safer and more robust method and biometrics are among the most reliable features that can be used in computer-aided personal recognition. Inconvenience with using the traditional methods caused a rapid increase in the application of biometrics. The most widely-used biometrics are fingerprints [1], facial features [2], iris patterns [3] and palmprints [4]. Palmprints provide a number of privileges over other biometric features, making them an appropriate choice for identification applications. First, they are more economical, as palmprint images can be easily obtained using inexpensive CCD cameras. Second, they are robust as hand features do not change significantly over time. Finally, palmprint-based systems work well in extreme weather and illumination conditions, since palmprints contain much richer set of features than most of other biometrics.

There are several useful features in a palm image such as line features (principal lines and wrinkles), geometrical features such as size of the palms, the angle between principal lines, textural features, etc.

Although line-based features are very useful in palmprint recognition, systems that work only based on these features face some problems. The first one is that in some cases principal lines and wrinkles are not enough to discriminate palms since there are many palms with similar line features. Fig.1 shows two palms with similar line pattern.

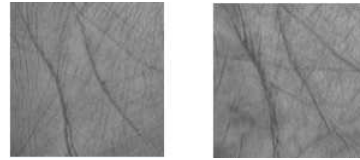


**Fig. 1.** Two different palms with similar principal lines

The second one is that in many cases palmprint lines are difficult to extract because of the low quality of images; two sample palmprint images of this kind are shown in Fig.2.

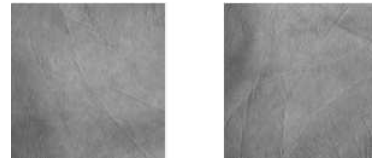


**Fig. 2.** Palmprints with unclear principal lines

One useful way to overcome these problems and to improve the accuracy of palmprint identification systems is to use multispectral imaging [5], which captures an image in a variety of spectral bands (in palmprint recognition usually four spectral bands are used). Each spectral band highlights specific features of the palm and helps us to derive more information from palmprint. So far, many approaches have been proposed for palmprint recognition. In [6], a survey of palmprint recognition systems is provided. The author has divided most of the previous algorithms into the following categories. There are some texture-based approaches (most of which used statistical methods for feature extraction). Many previous approaches are based features derived from transform domain

such as Gabor, Fourier and wavelet transform. As an example in [7], Han used a wavelet-based image fusion method for palmprint recognition. There are also some line-based approaches designed for palmprint recognition. Palm lines including principal lines and wrinkles are very useful features of palmprint. In [8], Wu proposed some line features and used them for palmprint matching. Some other methods used image coding techniques to perform palmprint recognition. In [9], Jia used a robust line orientation code for palmprint verification. Some other coding methods are also used for palmprint recognition, such as palm code, fusion code, competitive code, ordinal code [10]. In [11], Xu proposed a quaternion principal component analysis approach for multispectral palmprint recognition which achieved a high accuracy rate. Ekinci [12] proposed a Gabor wavelet representation approach followed by kernel PCA for palmprint recognition.

As discussed before, palm-line extraction could be difficult for some images. The origin of this difficulty lies in the similarity of the principal lines, reducing their discrimination capability from other palms. To overcome these problems we propose a hybrid feature that uses both the principal line information and also local wavelet energy of palms. This hybrid feature combines the following two features:

1. Principal lines and their energy in different locations of the palm.
2. Wavelet transform of palm image that can help us detect the small differences between different palms.

These two features are explained in more details in Section.2.1 and Section.2.2 respectively. In Section.3 we explain how to combine them in a proper way by scaling them in the same range. Section. 4 provides the experimental results of this algorithm on PolyU multispectral dataset [18] and Section.5 provides some conclusions.

## 2. PALMPRINT FEATURES

In this paper, we developed a recognition algorithm for multispectral palmprint images. Multispectral methods require different samples of the same object in order to make a better decision. Here we assume that in image acquisition section four images of each palmprint are acquired using four CCDs. These images are then preprocessed and the regions of interest (ROI) for each of them are extracted. Provided these RIOs, features are extracted from each palm. Basically we employ two parallel feature extraction paths and the final decision is concluded upon the results of the two paths. The two features used in this paper are local palm-line energy and local wavelet energy of palmprint. The basic idea is to divide palm images into a number of non-overlapping blocks and then find the energy of each blocks as its features.

### 2.1. Palm Line Extraction

As mentioned earlier, palmprints contain principal-lines and wrinkles that are exclusive to that palmprint. These lines are used in the palmprint identification literature for classification purposes, but extracting these lines accurately could be very difficult and in some cases impossible. Many methods are proposed to extract lines, such as Canny edge detection method, designing masks to compute first and second order derivatives of palm images, thresholding palm images to form binary edge images and then applying Hough transform, etc. Here we do not aim to extract lines precisely, instead we extract the region around each principal line and major wrinkles of the palm that contains the main characteristics of the palm. After extraction of these lines, we compute their energy in different parts of the image as local palm-line energy and use them as one set of features. The procedure for line extraction and finding their local energy can be divided into the following steps:

1. Smoothing the palm image with a Gaussian filter;
2. Extracting line edges;
3. Computing second order derivative of the palm;
4. Masking the smoothed image using the dilated version of the edge image;
5. Dividing the resulting image into  $T \times T$  non-overlapping blocks and computing the average energy of each block and stacking them to form the palm-line feature vector.

In the first step, palm image must be smoothed in order to reduce the effect of noise. One possible approach for image smoothing is to apply a Gaussian filter. The discrete 2D Gaussian filter is defined as:

$$G(m, n) = \frac{1}{2\pi\sigma^2} e^{-\left(\frac{(m-\mu_x)^2}{2\sigma_x^2} + \frac{(n-\mu_y)^2}{2\sigma_y^2}\right)}$$

We can convolve this filter with the palm image to derive a smoothed version of palmprint. The result of applying the Gaussian filter to the original image,  $I$ , at pixel  $(m, n)$  can be computed as:

$$P(m, n) = \sum_{s=-a}^a \sum_{t=-b}^b M(s, t) I(m + s, n + t)$$

The above filter has a number of parameters to be set; We use a Gaussian filter with zero mean and unit variance. Moreover, mask dimensions are two other parameters to be set. Here we used a square mask of size  $7 \times 7$  ( $a=b=3$ ), which was chosen experimentally on a training set. Fig.3 depicts the smoothed image.

Having the smoothed image, edges of the principal lines must be extracted. Here Sobel edge detection algorithm is used. After applying Sobel mask, there will be some isolated points which need to be eliminated. To remove them, an

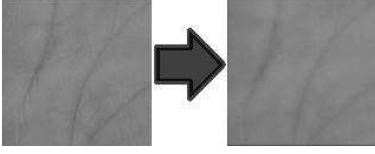


**Fig. 3.** Smoothed palm image

isolated point removal algorithm is used. For every nonzero pixel, we look at its neighborhood of 3 by 3 and if the number of adjacent nonzero pixels is less than 3 we remove that pixel. The resulting edge image is shown in Fig.4.

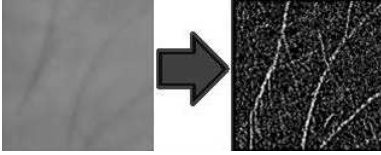


**Fig. 4.** Edges of the palm

In the third step, second order derivative of the palm image is computed. Pixels with positive values are kept. The reason being the pixels at principal line locations have darker values than their surrounding pixels, and the second order derivative often has its maximum values at these points. Fig.5 depicts the result of this step.

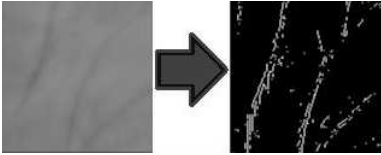


**Fig. 5.** Second order derivative of palm

In the forth step, the morphological dilation is used to expand the region around edges in images of previous steps. Then the images of step 2 and 3 are multiplied resulting in an image containing major lines and wrinkles. Fig.6 denotes the result of major line extraction. As it can be seen not all principal lines are extracted, and some of the extracted lines are not connected. But for our feature extraction this level of accuracy is good enough.

In the fifth step, the resulting image from previous step is divided into non-overlapping blocks and average energy of each block is computed. Then we stack the average energy of different blocks to form the palm-line feature vector of each image. As mentioned earlier, there are 500 different palms in the database. Let us denote the palmsprints matrices by  $P_1$  to  $P_{500}$ . For each palm, there are 12 sample images in four spectrum bands (red, green, blue, NIR). Concatenating all of these twelve sample images in together we get  $P_i$  as:

$$P_i = [P_{i1}|P_{i2}|...|P_{i,12}] \quad \text{for } i = 1 : 500$$

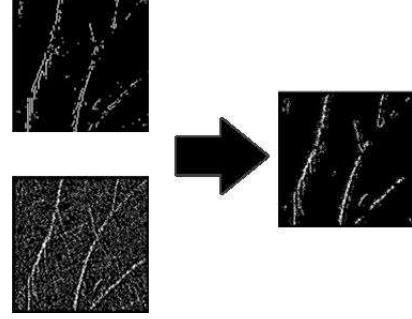


**Fig. 6.** combination of edge image and second order derivative of palm

Any of the  $P_{ij}$ 's consists of four images in four different spectra. We denote the red, green, blue and NIR components with  $R_{ij}, G_{ij}, B_{ij}$  and  $N_{ij}$  matrices. So  $P_{ij}$  can be shown as:

$$P_{ij} = [R_{ij}|G_{ij}|B_{ij}|N_{ij}]$$

Each of  $R_{ij}, G_{ij}, B_{ij}, N_{ij}$  is a 128 by 128 matrix, so  $P_{ij}$  is a 128 by 512 matrix. After extracting palmlines, we divide each of  $R_{ij}, G_{ij}, B_{ij}, N_{ij}$  to 4 by 4 non-overlapping blocks. So each of these matrices is divided into 1024 sub-matrices. We number these sub-matrices from 1 to 1024 as it is shown in Fig.7.

1	33	...	993
2	34	...	994
...	...	...	...
32	64	...	1024

**Fig. 7.** matrix numbering

Then the feature vector of each spectrum, for example red spectrum, can be derived as:

$$f_L(R_{ij}) = [f_L^1(R_{ij}), f_L^2(R_{ij}), ..., f_L^{1024}(R_{ij})]$$

Where  $f_L^k(R_{ij})$  denotes the average palm-line energy in the k-th block (the subscript  $L$  stands for line feature) and can be computed as:

$$f_L^k(R_{ij}) = \frac{1}{16} \sum_{\substack{\text{for all} \\ (m,n) \in R_{ij}^{(k)}}} p(m,n)^2$$

and  $p(m,n)$  denotes pixel value of the image at the position  $(m,n)$ .

Now the feature of other spectra,  $G_{ij}, B_{ij}$  and  $N_{ij}$ , can also be extracted using the same approach. At the end the feature vector of these four spectra are concatenated to form the final palm-line energy feature of each palmprint which has a length of 4048 and can be shown as:

$$f_L(P_{ij}) = [f_L(R_{ij})|f_L(G_{ij})|f_L(B_{ij})|f_L(N_{ij})]$$

## 2.2. Wavelet Features

The discrete wavelet transform (DWT) is used in a variety of signal processing applications, such as video compression [13], image denoising [14], image inpainting [15], etc. Unlike the Fourier transform, whose basis functions are sinusoids, wavelet transform is based on small waves, called wavelets, of varying frequency and limited duration. DWT can efficiently represent some signals, especially ones that have localized changes.

Here, we use wavelet transform for extracting features from palmprint images. The Daubechies-2 wavelet (db2) is applied up to 3 stages to palm images from all the four spectra and the energy of each subband is calculated locally and used as one feature. This method can be summarized in the following steps:

1. Apply wavelet transform to each palm image up to 3 levels;
2. Divide each subband image into  $T \times T$  non-overlapping blocks;
3. Compute the average energy of each block and concatenate them to form local wavelet feature vector.

Fig.8 depicts a 3-level wavelet decomposition result.

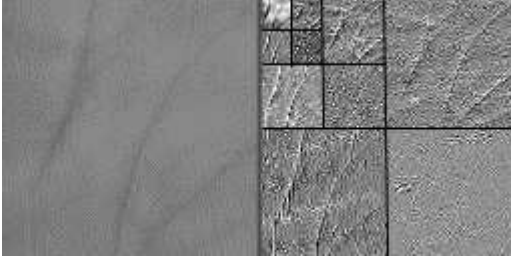


**Fig. 8.** (a) palm image (b) 3-level wavelet decomposition

It is worth to mention that the LLL subband is not used in wavelet feature derivation step. But all other subbands are used. To provide more details on how the wavelet features are derived, let us assume we want to derive the wavelet features from  $j$ -th sample of  $i$ -th person. This is shown by  $P_{ij}$  and defined as:

$$\mathbf{P}_{ij} = [\mathbf{R}_{ij} | \mathbf{G}_{ij} | \mathbf{B}_{ij} | \mathbf{N}_{ij}]$$

We first need to derive the wavelet transform for all four components up to three stages,  $\mathbf{R}_{ij}$ ,  $\mathbf{G}_{ij}$ ,  $\mathbf{B}_{ij}$  and  $\mathbf{N}_{ij}$ . For each of them we will use 9 wavelet subbands for feature extraction (all subbands except LLL). We divide each subband into 64 blocks and calculate the average energy of any of those blocks and we put them in a  $64 \times 9$  dimensional vector. This feature vector can be shown as below:

$$\mathbf{f}_w(R_{ij}) = [\mathbf{w}_{R_{ij}}^{(1)} | \mathbf{w}_{R_{ij}}^{(2)} | \dots | \mathbf{w}_{R_{ij}}^{(576)}]$$

The wavelet features of  $\mathbf{G}_{ij}$ ,  $\mathbf{B}_{ij}$  and  $\mathbf{N}_{ij}$  can also be derived in the same way as  $\mathbf{R}_{ij}$ . Then the feature vector of  $\mathbf{P}_{ij}$  is formed by concatenation of features of all four spectra and denoted as:

$$\mathbf{f}_w(P_{ij}) = [\mathbf{f}_w(R_{ij}) | \mathbf{f}_w(G_{ij}) | \mathbf{f}_w(B_{ij}) | \mathbf{f}_w(N_{ij})]$$

## 3. CLASSIFICATION ALGORITHM FOR IDENTIFICATION

After extraction of the features of all people in the dataset, a classifier needs to be used to find the closest match of each test sample. There are different classifiers which can be used for this task including neural networks [16], support vector machine (SVM) [17] and minimum distance classifier. In this work minimum distance classifier is used which is popular in biometric recognition area. Minimum distance classifier basically matches a new test sample to a class with the closest distance between their feature vectors.

Suppose we want to identify the class label of a sample palmprint shown as  $P_x$ . We first need to find the Euclidean distance of its feature vector with all training samples in dataset. Then the predicted class label,  $k^*$ , for this palmprint can be found as:

$$k^* = \underset{k}{\operatorname{argmin}} [\operatorname{dis}(P_x, P_k)]$$

where  $\operatorname{dis}(P_x, P_k)$  is defined as the summation of normalized distance of line features and wavelet features as is defined as:

$$\operatorname{dis}(P_x, P_k) = \operatorname{dis}^{(n)}(\mathbf{f}_L(P_x), \mathbf{f}_L(P_k)) + \operatorname{dis}^{(n)}(\mathbf{f}_w(P_x), \mathbf{f}_w(P_k))$$

where  $\operatorname{dis}^{(n)}$  denotes the normalized distance between corresponding features vectors and defined as:

$$\operatorname{dis}^{(n)}(\mathbf{f}_L(P_x), \mathbf{f}_L(P_k)) = \|\mathbf{f}_L(P_x) - \mathbf{f}_L(P_k)\| / \bar{d}_L$$

$$\operatorname{dis}^{(n)}(\mathbf{f}_w(P_x), \mathbf{f}_w(P_k)) = \|\mathbf{f}_w(P_x) - \mathbf{f}_w(P_k)\| / \bar{d}_w$$

and  $\bar{d}_L$  and  $\bar{d}_w$  are normalization factors and are derived as:

$$\bar{d}_L = \sum_{k=1}^{500} \|\mathbf{f}_L(P_x) - \mathbf{f}_L(P_k)\|, \quad \bar{d}_w = \sum_{k=1}^{500} \|\mathbf{f}_w(P_x) - \mathbf{f}_w(P_k)\|$$

The reason for normalizing the distances is that, the palm-line and wavelet features have different range and if we simply add them together, one of them might dominate the other one by having larger range. Despite the simplicity of the minimum distance classifier, it achieves very high recognition accuracy in our system. We need to mention that the feature vector for the  $i$ -th person in the training set is defined as the average feature vector of different training images of that person and can be computed using the following equation :

$$\mathbf{f}_w(P_i) = \frac{\sum_{j=1}^M \mathbf{f}_w(P_{ij})}{M}$$

#### 4. RESULTS

We have tested our identification algorithm on a well-known multispectral palmprint database known as PolyU database [18], containing 6000 palmprints captured from 500 different palms. Every palm was sampled 12 times within different times. So there are  $12 \times 500 = 6000$  palmprint images. Every image was taken under 4 spectra, including Red, Green, Blue and NIR (Near Infra-Red). These images have a resolution of  $128 \times 128$ . Four sample palmprints from this dataset are shown in Fig.9.

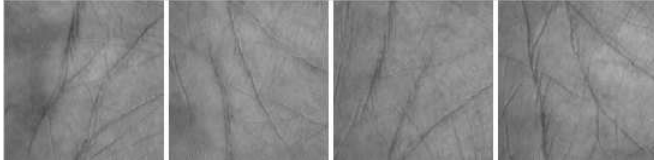


**Fig. 9.** Four sample palmprints

Correct identification takes place when a test palmprint is classified as the right person and misidentification takes place when the palmprint is classified into a category whose label is different from its actual label. In our first experiment, half of the images from each group are used as training samples (in this experiment, the first six samples in each palm image are selected for training) and the remaining images are used as test samples. Among all 3000 palmprints in the database, 14 samples were misidentified; So the identification accuracy is about 99.53%.

To make the experiment fair, we performed another experiment. For each person we select six palm images randomly as training samples, and test on the other samples. We repeat this procedure ten times and compute the final accuracy rate by averaging on the accuracy rate of all experiment. So, the number of test samples in this experiment is 30000. In this experiment an accuracy rate of 98.8% is obtained.

In another experiment we examined the effect of the number of training samples on the accuracy rate ( in these experiments we select the training samples randomly and repeat the experiment ten times). We calculated the accuracy of the proposed scheme using different number of training samples, from 4 to 6, and found out reducing the number of training examples does not decrease the accuracy rate significantly. This is very desirable for the cases where the training data is small. The result of this experiment is shown in Table 1.

We have also provide a comparison of the proposed scheme with two earlier approaches on this dataset. One of them being the PCA+GWR approach which uses a Gabor wavelet representation approach followed by kernel PCA, and the other one being QPCA, which uses a quaternion principal component analysis approach for multispectral palmprint recognition. This comparison is provided in Table 2.

**Table 1.** accuracy rate of proposed method based on number of training samples

Ratio of training sample	Number of test samples	accuracy using line features	accuracy using wavelet features	accuracy using both features
6/12	30000	94.58%	98.49%	98.88%
5/12	35000	93.87%	98.25%	98.45%
4/12	40000	93.22%	97.81%	98.08%

**Table 2.** Comparison with other algorithms for palmprint recognition

Training ratio	PCA+GWR [12]	QPCA [11]	Proposed approach
6/12	95.17%	98.13%	98.88%

#### 5. CONCLUSION

This paper proposed a hybrid feature for palmprint recognition. The proposed hybrid feature combines two sets of features, palm-line features and wavelet features. The palm-lines are extracted by applying a Laplacian mask on the smoothed image and the wavelet features are derived from local wavelet subbands of image after applying wavelet transform up to three stages. We then use minimum distance classifier to perform template matching. Using this hybrid feature, our algorithm is able to identify palmprints with similar line patterns and unclear palmprints. We have performed an experiment to evaluate the effect of reducing the ratio of training to test samples and it turns out the recognition accuracy will not change too much by reducing the training ratio, makes this algorithm desirable for cases where the amount of training data is limited. This algorithm can also be used for other biometric recognition tasks.

#### Acknowledgments

The authors would like to thank biometric research group at PolyU hong kong for providing the fingerprint dataset.

#### 6. REFERENCES

- [1] D. Maltoni, D. Maio, A.K. Jain and S. Prabhakar, "Handbook of fingerprint recognition," Springer Science and Business Media, 2009.
- [2] W. Zhao, R. Chellappa, P.J. Phillips and A. Rosenfeld, "Face recognition: A literature survey," ACM Computing Surveys (CSUR) 35, no. 4: 399-458, 2003.
- [3] K.W. Bowyer, K.P. Hollingsworth and P.J. Flynn, "A survey of iris biometrics research: 2000-2010," Handbook of iris recognition. Springer London, 15-54, 2013.

- [4] S. Minaee, A.A. Abdolrashidi, "Multispectral palmprint recognition using textural features," IEEE Signal Processing in Medicine and Biology Symposium, 2014.
- [5] D. Zhang, Z. Guo, G. Lu, L. Zhang and W. Zuo, "An Online System of Multi-spectral Palmprint Verification", IEEE Transactions on Instrumentation and Measurement, vol. 59, no. 2, pp. 480-490, 2010.
- [6] A. Kong, D. Zhang and M. Kamel, "A survey of palmprint recognition." Pattern Recognition 42.7: 1408-1418, 2009.
- [7] D. Han, Z. Guo and D. Zhang, "Multispectral palmprint recognition using wavelet-based image fusion." IEEE International Conference on Signal Processing, pp. 2074-2077, 2008.
- [8] X. Wu, K. Wang, D. Zhang, "Line feature extraction and matching in palmprint,"Proceeding of the Second International Conference on Image and Graphics, pp. 583-590, 2002.
- [9] W. Jia, D.S. Huang, and D. Zhang, "Palmprint verification based on robust line orientation code," Pattern Recognition, 41(5):1504-1513, 2008.
- [10] F. Yue, W.M. Zuo, and D. Zhang, "FCM-based orientation selection for competitive code-based palmprint recognition," Pattern Recognition, 42(11):2841-2849, 2009.
- [11] X. Xu and Z. Guo, "Multispectral palmprint recognition using quaternion principal component analysis," IEEE Workshop on Emerging Techniques and Challenges for Hand-Based Biometrics, pp. 15, 2010.
- [12] M. Ekinici and M. Aykut, "Gabor-based kernel PCA for palmprint recognition," Electronics Letters, vol. 43, no. 20, pp. 1077-1079, 2007.
- [13] A. Skodras, C. Christopoulos and T. Ebrahimi, "The JPEG 2000 still image compression standard." Signal Processing Magazine, IEEE 18.5: 36-58, 2001.
- [14] SG. Chang, B. Yu, M. Vetterli, "Adaptive wavelet thresholding for image denoising and compression." Image Processing, IEEE Transactions on 9.9: 1532-1546, 2000.
- [15] B. Dong, H. Ji, J. Li, Z. Shen, Y. Xu, "Wavelet frame based blind image inpainting," Applied and Computational Harmonic Analysis 32, no. 2: 268-279, 2012.
- [16] M. Anthony, P.L. Bartlett, "Neural network learning: Theoretical foundations," cambridge university press, 2009.
- [17] C. Cortes and V. Vapnik, "Support-vector networks," Machine learning 20, no.3: 273-297, 1995.
- [18] <http://www.comp.polyu.edu.hk/biometrics/HRF/HRF.htm>